

Break-Junction Tunneling on MgB₂

H. Schmidt,^{1,2} J. F. Zasadzinski,^{1,2} K. E. Gray,¹ and D. G. Hinks¹

¹*Materials Science Division, Argonne National Laboratory, Argonne, IL 60439*

²*Physics Division, Illinois Institute of Technology, Chicago, IL 60616*

(Dated: March 7, 2019)

Tunneling data on magnesium diboride, MgB₂, are reviewed with a particular focus on superconductor–insulator–superconductor (SIS) junctions formed by a break–junction method. The collective tunneling literature reveals two distinct energy scales, a large gap, $\Delta_L \sim 7.2$ meV, close to the expected BCS value, and a small gap, $\Delta_S \sim 2.4$ meV. The SIS break junctions show clearly that the small gap closes near the bulk critical temperature, $T_c = 39$ K. The SIS spectra allow proximity effects to be ruled out as the cause for the small gap and therefore make a strong case that MgB₂ is a coupled, two–band superconductor. While the break junctions sometimes reveal parallel contributions to the conductance from both bands, it is more often found that Δ_S dominates the spectra. In these cases, a subtle feature is observed near $\Delta_S + \Delta_L$ that is reminiscent of strong–coupling effects. This feature is consistent with quasiparticle scattering contributions to the interband coupling which provides an important insight into the nature of two–band superconductivity in MgB₂.

PACS numbers: PACS numbers: 73.40.Gk, 74.50.+r, 74.70.Ad, 74.80.Fp

INTRODUCTION

Approximately one and a half years after the discovery [1] of superconductivity in MgB₂ a wealth of information about its properties has been collected. While its high critical temperature and simple crystal structure generated an initial flurry of activity, there is now an increasing interest in the nature of superconductivity in MgB₂, as it appears to be one of the rare examples of a two–band superconductor.

Theoretically, such two–band behavior was proposed for MgB₂ because the electronic system consists of two qualitatively different types of charge carriers, derived from boron π – and σ –bands, respectively [2]. The π –bands are three dimensional (3D), while the σ –bands are effectively restricted to two dimensions (2D). For convenience, these actual four bands are henceforward treated as two effective bands. Superconductivity is proposed to arise from electron–phonon coupling of the 2D band with a specific boron bond–stretching mode. That implies, that superconductivity originates from the σ –band and that superconductivity in the π –band is driven by that primary interaction. As a result, the properties of superconductivity are proposed to be different in both bands, provided the material is in the clean limit and the electronic systems do not strongly mix. The 2D band shows a large gap, $\Delta_L \sim 7.2$ meV, whereas the 3D band shows a small gap, $\Delta_S \sim 2.4$ meV, both closing at a joint critical temperature, T_c . In the dirty limit, only one gap of intermediate magnitude is expected to be observed, closing at a reduced T_c .

There now is sufficient experimental evidence to strongly support such a two–band scenario, and there is a growing consensus in the community to this end. However, a large fraction of these experiments involved tunneling spectroscopy which is susceptible to surface imper-

fections. Specifically, surface proximity effects can mimic the effects of two–band superconductivity. In this paper, we will present an overview of tunneling results, and will use this together with our own experimental data to argue in favor of the two–band nature of superconductivity in MgB₂.

TECHNIQUES OF TUNNELING SPECTROSCOPY

Tunneling spectroscopy traditionally presents one of the most direct probes of the superconducting energy gap [3]. In superconductor–insulator–normal metal (SIN) tunnel junctions, the conductance at low temperature is equivalent to the density of states (DOS) near the Fermi energy, E_F . At finite temperature, the conductance may be calculated from:

$$\frac{dI}{dV} = -\sigma_N \int N(E) \frac{\partial f(E + eV)}{\partial eV} dE, \quad (1)$$

where N_S is the superconducting DOS and σ_N the conductance of the junction in the normal state. To account for experimentally observed broadening in excess of thermal smearing, a smearing parameter Γ usually is introduced into the BCS DOS [4]:

$$N(E) = \Re \frac{E - i\Gamma}{\sqrt{(E - i\Gamma)^2 - \Delta^2}}. \quad (2)$$

A widely used realization of such SIN junctions is the scanning tunneling microscope (STM), where the barrier is given by a short length of vacuum that separates the STM tip from the sample. This technique combines an ideal insulating barrier with high spatial resolution. On the other hand, quite frequently a tip is placed into direct contact to the sample, a setup generally known as

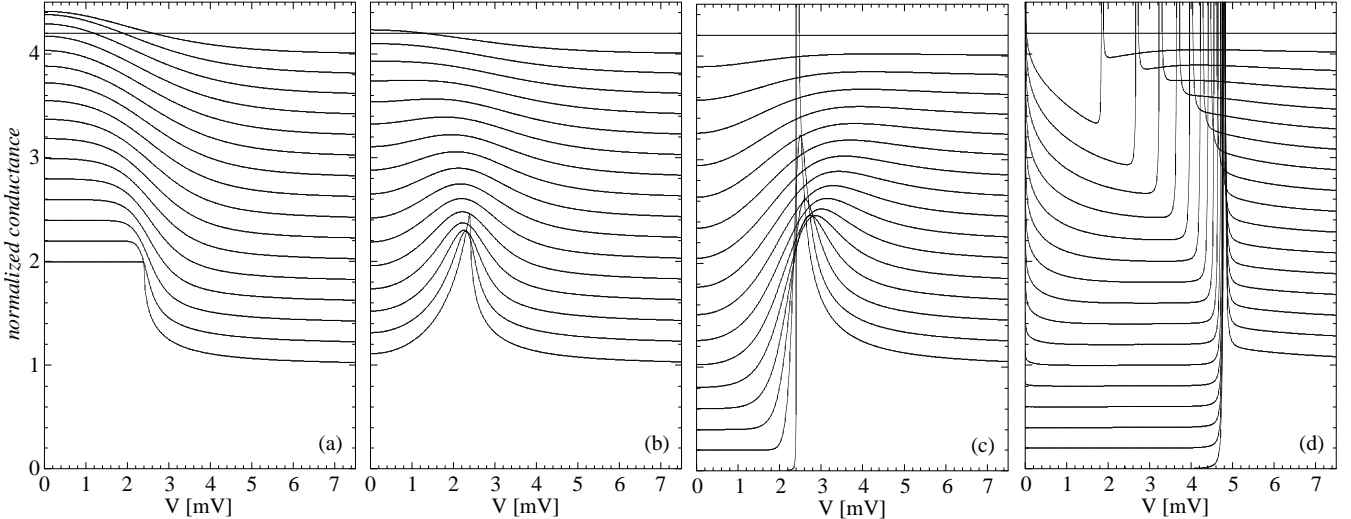


FIG. 1: Simulated temperature dependence of (a) an SIN junction with $Z = 0$ (purely metallic), (b) $Z = 0.5$ (intermediate), (c) $Z \rightarrow \infty$ (pure tunneling) and (d) an SIS tunnel junction. Parameters used are: $\Delta_0 = 2.4$ meV and $T_c = \frac{\Delta_0}{1.76k_B} = 15.8$ K. Curves are vertically shifted for clarity, temperature increment is 1 K. To avoid singularities, $\Gamma = 1$ μ eV was included (using the formalism described in Ref. [7] for (a) and (b)).

point contacts. Such systems usually lack fine spatial resolution, but they allow for a significantly lower contact resistance and can be used to realize a continuous transition from a tunnel junction (insulating barrier) to a metallic contact (no barrier). Metallic contacts show enhanced current at bias voltages lower than the superconducting energy gap due to Andreev reflections [5], and hence they also allow one to determine the energy gap. In the intermediate case, both tunneling and Andreev reflections contribute to the transport over the barrier, a case that was analytically described by Blonder, Tinkham and Klapwijk (BTK) [6].

Finally, symmetrical SIS junctions display very sharp features at twice the energy gap, that are a result of the convolution of two BCS DOSs:

$$I = \frac{\sigma_N}{e} \int N(E)N(E + eV)[f(E) - f(E + eV)]dE. \quad (3)$$

Such SIS junctions may be used to study the energy gap and a major advantage is their ability to trace the gap feature to highest temperatures, as the coherence peaks prove to be fairly insensitive against thermal smearing.

To demonstrate this, Fig. 1 compares the temperature evolution of simulated spectra assuming a 2.4 meV BCS superconductor with insignificant smearing ($\Gamma = 1$ μ eV), for (a) a purely metallic, (b) an intermediate and (c) a pure tunnel junction, as well as (d) a symmetric SIS tunnel junction. Not only do the coherence peaks remain sharp up to highest temperatures in the SIS case, they furthermore directly scale with the closing of the gap. In comparison, the peak position in the SIN tunneling case increases as T approaches T_c —even though the gap actually closes. A close relation between the SIS coherence

peak position and $\Delta(T)$ is preserved even in the presence of significant smearing. We will make use of this peculiarity to precisely measure $\Delta_S(T)$.

EXPERIMENT

A tremendous amount of tunneling work has been performed on MgB₂, and even though such a narrow view certainly does not mirror the full depth of information obtained from these studies, we for now want to focus only on the inferred energy gap values. Table I gives a compilation of these values, and it immediately becomes evident that most studies agree with the presence of two gaps around $\Delta_S = 2.0\text{--}2.8$ meV and $\Delta_L = 7.0\text{--}7.5$ meV. This observation of two gaps, as well as their values, are in nice agreement with theoretical predictions [2, 61, 62], however, some more effort is needed to positively confirm two-band superconductivity as the origin of these features.

Tunneling spectroscopy by nature is a surface probe and it is important to carefully verify that its results represent the bulk properties of the sample. Degraded surfaces were repeatedly suggested as an origin for small gap values [39], and there still are some lingering concerns as to whether multiple gaps in tunneling are “real”. To answer to that, more information than the mere gap values is needed, and tunneling can readily supply such information.

The polycrystalline samples used in the present work were prepared as described in Ref. [41]. Tunneling spectra were taken using a home-built point-contact apparatus and a Au tip [63]. This resulted in both SIN and

Experiment	Energy Gap / [meV]		Reference
STM	$\Delta_S = 2.0$		[8, 9]
		$\Delta = 5 - 7$	[10, 11]
	$\Delta_S = 2.3$	$\Delta_L = 7.1$	[12, 13, 14, 15]
	$\Delta_S = 3.5$	$\Delta_L = 7.5$	[16, 17, 18]
	$\Delta_S = 2.2$	$\Delta_L = 6.9$	[19, 20]
	$\Delta_{xy} = 5.0$	$\Delta_z = 8.0$	[21]
Point Contact	$\Delta_S = 2.6$		[22]
	$\Delta_S = 1.7$	$\Delta_L = 7$	[23]
	$\Delta_S = 3$	$\Delta_L = 7$	[24]
	$\Delta_S = 2.8$	$\Delta_L = 9.8$	[25, 26]
	$\Delta_S = 2.8$	$\Delta_L = 7.0$	[27]
	$\Delta_S = 2.45$	$\Delta_L = 7.0$	[28, 29, 30]
	$\Delta_S = 2 - 3$	$\Delta_L = 6 - 8$	[31]
	$\Delta_S = 2.3$	$\Delta_L = 6.2$	[32]
		$\Delta = 3 - 4$	[33]
	$\Delta_S = 2.7$	$\Delta_L = 7.1$	[34]
Break Junction	$\Delta_S = 2.8$	$\Delta_L = 7.1$	[35, 36, 37]
	$\Delta_S = 1.7 - 2$		[37, 38]
	$\Delta_S = 2.5$	$\Delta_L = 7.6$	[39, 40, 41, 42]
	$\Delta_S = 2 - 2.25$	$\Delta_L = 8.5 - 9.5$	[43]
	(SQUID)	$\Delta_S = 2.02$	[44]
Planar Junction		N/A	[45, 46]
	Step-Edge	$\Delta_S = 2.0$	N/A
	Ramp	$\Delta_S = 2.0$	N/A
	Nanobridge	(SQUID)	N/A
	Trench	(SQUID)	N/A
Sandwich	Metal Masked Ion Damage		N/A
	MgB ₂ /Ag		$\Delta_L = 7.3$
	MgB ₂ /Pb	$\Delta_S = 1.75$	$\Delta_L = 8.2$
	MgB ₂ /Al/Al ₂ O ₃ /Nb	$\Delta_S = 2.2$	
	MgB ₂ /AlN/NbN	$\Delta_S = 2.95$	
	MgB ₂ /MgO _x /Au, Ag	$\Delta_S = 2.5$	

TABLE I: Energy gaps of MgB₂ inferred from different tunneling experiments in the literature. Experiments are listed by technique as well as they are sorted by research group. For each group, only the most recent findings are given. For reference, all tunneling studies are listed, including a few that did not determine any energy gap value.

SIS junctions, however, henceforward we will focus on the SIS break junctions.

TEMPERATURE DEPENDENCE OF Δ_S

The first unexpected result from tunneling spectroscopy on MgB₂ was the observation of a small energy gap, $\Delta_S = 2.0$ meV [8], much smaller than the weak coupling limit would allow for $T_c = 39$ K. The simplest scenario to result in a reduced gap value is a surface layer of reduced superconductivity with a gap anywhere in between the bulk value and zero. This scenario can posi-

tively be ruled out by studying the temperature dependence of the small gap, since such a reduced gap should still scale with the local, reduced T_c , i.e. it should obey $\frac{2\Delta_0}{k_B T_c} \geq 3.52$ [70]. This is illustrated in Fig. 2, where schematically the temperature dependence of an intrinsic small gap is compared with the expectation for Δ_S in a coupled two-band model.

For this reason, $\Delta_S(T)$ was measured in a number of tunneling studies, and it was concluded to close at or near the bulk T_c of 39 K. However, the unusual combination of a small gap and high temperatures results in significant smearing in SIN junctions that renders the determination of $\Delta_S(T)$ more difficult. In cases where two

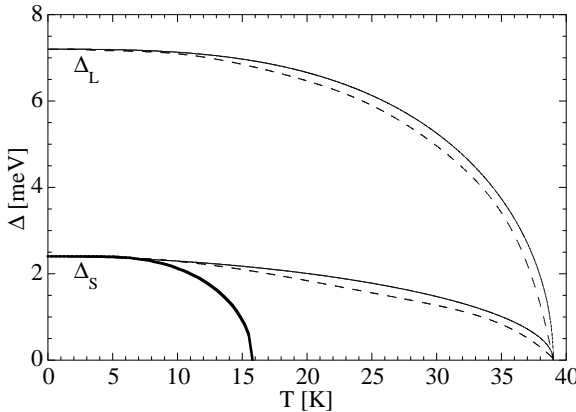


FIG. 2: Temperature dependence for an uncoupled small gap (heavy line, which was used to compute Fig. 1) as compared to a small, coupled gap (thin line after Ref. [62], dashed line after Ref. [2]).

gaps are observed simultaneously the exact analysis of high-temperature data is further complicated. SIS junctions promise to provide a solution to this problem, as they are insensitive to thermal smearing.

The evolution of SIS conductance spectra with temperature (Fig. 1d) also allows a clear identification of a junction as being SIS type, whereas the low-temperature data might be inconclusive. To illustrate this, Fig. 3 shows a junction that originally was interpreted in terms of SIN tunneling using $\Delta = 4.1$ meV and no smearing, but no temperature dependent data was taken [39, 40]. This fit is compared to an SIS model using $\Delta = 2.3$ meV and $\Gamma = 0.4$ meV, parameters that are now established to be typical for MgB_2 . Based only on the low-temperature data, a conclusive decision is difficult, as both fits, though different in detail, capture the major features of the data (with the exception of the zero-bias peak).

Figure 4 finally shows the temperature dependence for

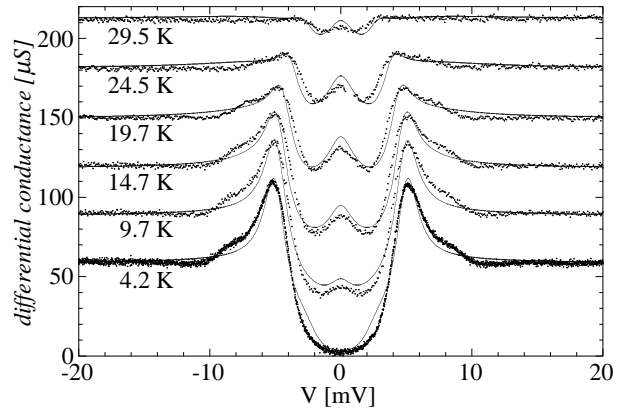


FIG. 4: Temperature dependence of an SIS spectrum showing exclusively the small gap [41].

such a junction. Even at high temperature, a clearly developed gap structure is visible in the raw data, which together with the obvious closing of the peak position along with the closing of the gap is conclusive evidence of the SIS nature of this junction. To further analyze such data, a simple BCS SIS model was employed, where Γ was adjusted to best fit the lowest temperature data and then held constant with increasing temperature, leaving Δ_S the only parameter used to adjust the fits to higher temperature data. These fits closely reproduce the evolution of (i) the peak height, (ii) the zero bias conductance peak caused by thermally activated current and (iii) the filling of the gap due to thermal smearing. This establishes the validity of such a simple model to exactly determine $\Delta_S(T)$ from this data.

The results of such fits, performed on three different junctions, are shown in Fig. 5. The small error bars represent the uncertainty in fitting the data, and there is excellent reproducibility among the three sets of data. This evolution of Δ_S closely resembles the theoretical

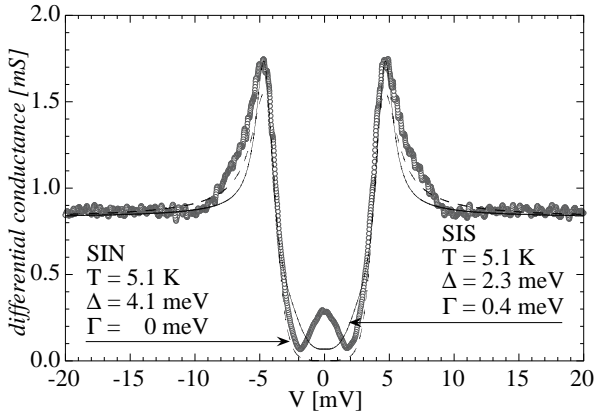


FIG. 3: Low temperature conductance spectrum (symbols) taken from Ref. [39] along with fits to an SIN (dashed line) and an SIS model (solid line).

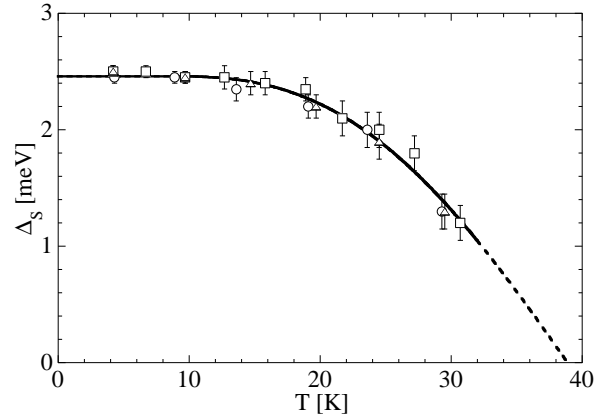


FIG. 5: Temperature evolution $\Delta_S(T)$ from BCS fits to three independent sets of data [41].

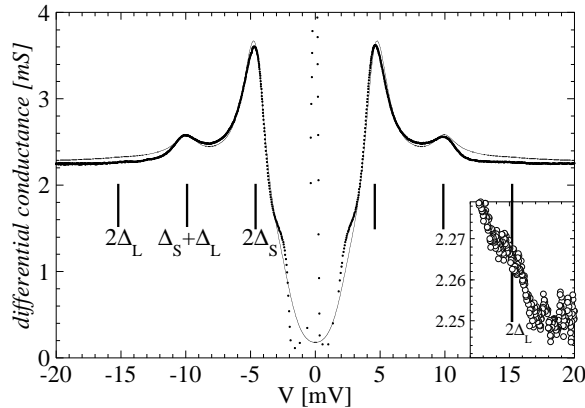


FIG. 6: Conductance spectrum showing direct current contribution from the 2D band along with a fit to an SIS model using a weighted sum of two BCS DOSs. Inset shows high bias on an expanded y-scale. The sharp zero-bias peak reflects a Josephson current in this low-resistance junction.

prediction (see Fig. 2) for a two-band model, and is incompatible with this gap being an isolated order parameter, as $\frac{2\Delta_0}{k_B T_c}$ would be significantly lower than the weak-coupling limit. This temperature dependence thus gives direct evidence for the presence of a second, larger order parameter, although typically no contribution from the second, 2D band is observed in SIS data.

SPECTROSCOPY OF Δ_L

Such current contributions from the 2D band are expected to show up at $eV = \Delta_L$ in SIN junctions and at $\Delta_S + \Delta_L$ and $2\Delta_L$ in SIS junctions. However, it is necessary to very carefully analyze whatever extra features are observed. Both the spectra in Fig. 6 and Fig. 7a, respectively, show additional features at bias close to $\Delta_S + \Delta_L$, yet the shape of these features is entirely different. Whereas in the first case a distinct peak is observed, the second spectra displays a dip at about the same position.

The extra peak in Fig. 6 can easily be attributed to direct tunneling contributions from the 2D band. The relative weight of such contributions depends on the density of charge carriers in the respective bands (the 3D band accounts for 58% of the total DOS [2]), and the orientation of the junction. Since the small gap is hosted in a 3D band, it is expected to contribute to junctions of any given orientation, whereas the large gap requires the junction to be aligned with the 2D bands which generally will not be the case. We believe, that the latter condition is crucial for the observed dominance of the small gap.

Figure 6 gives an example for the rare case that such alignment is achieved in SIS break junctions. Two clearly developed peaks are visible in the spectrum, that can be ascribed to 3D–3D and 3D–2D tunneling. Note again the

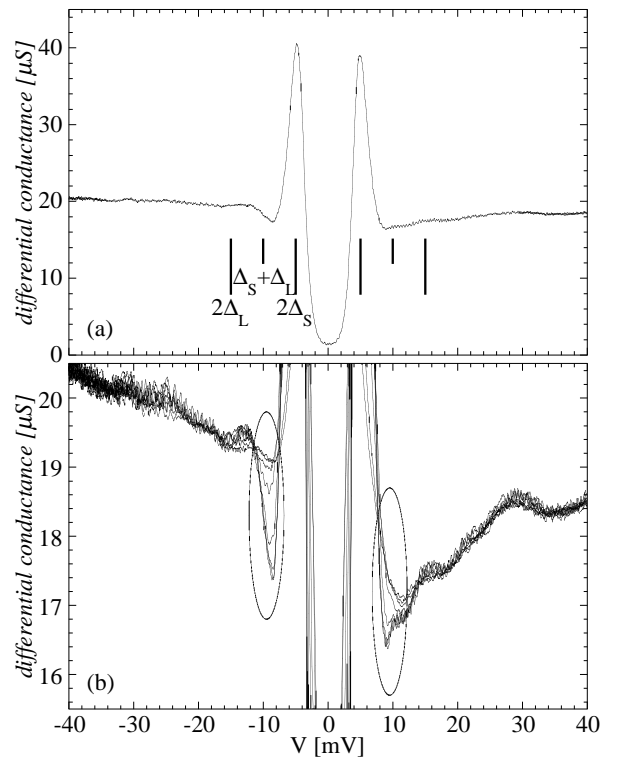


FIG. 7: (a) Low temperature spectrum showing a clearly developed dip structure near $\Delta_S + \Delta_L$. (b) Evolution of the background with increasing field (0 – 1.4 T with a 0.2 T increment). The encircled $\Delta_S + \Delta_L$ -structure vanishes with increasing field.

qualitative difference between this second peak and the $\Delta_S + \Delta_L$ -dip feature that will be discussed below.

To fit this data, we use BCS DOSs for both bands, adjusting the gap magnitudes to fit the well developed coherence peaks and choosing the mixing ratios in both electrodes to reproduce the observed peak heights. Such a model yields $\Delta_S = 2.3$ meV and $\Delta_L = 7.6$ meV, consistent with our previous data (in the case of Δ_S) as well as with other experimental reports.

The fit shown in Fig. 6 uses weights of 2 and 4%, respectively, for the large gap contribution in the two electrodes [71]. While the gap magnitudes (which contain the important, intrinsic information) are well-defined from the data, this is not the case for these mixing ratios, as there is no reason to assume them to be equivalent in both electrodes. The presence of the second peak gives evidence for contributions to the total current from the 2D band in at least one electrode, however, it does not give evidence as to how this 2D contribution is distributed over both electrodes. In principle, only one electrode needs to show alignment with the 2D band to produce a second peak at $\Delta_S + \Delta_L$. The decisive information would be the presence of a third peak at $2\Delta_L$, however, its amplitude is expected to be negligible unless the 2D band contributions are significant *in both electrodes*.

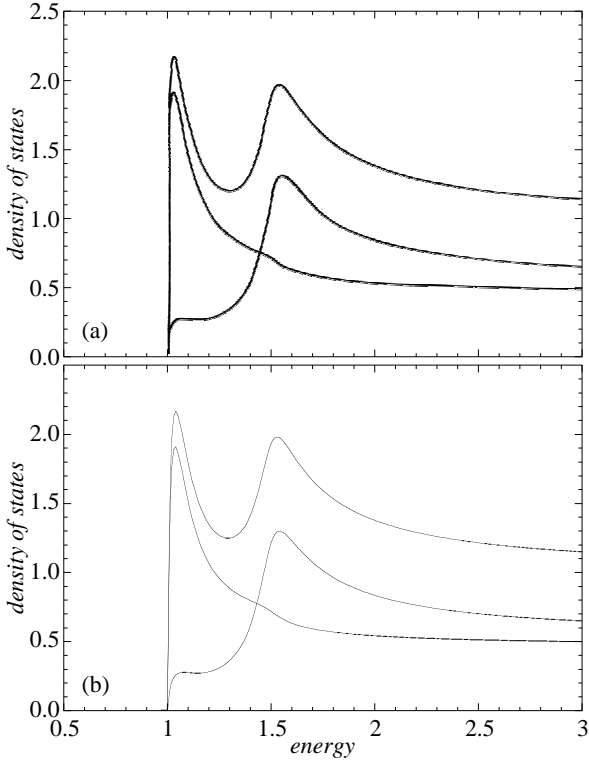


FIG. 8: (a) Partial and total DOS in a full two-band model (reprinted from Ref. [65], Fig. 3, copyright 1977, with permission from Elsevier Science). (b) Equivalent DOS calculated using McMillan's tunneling model of the proximity effect.

[72]. We checked our data for such a third peak and find a *very* weak shoulder at the corresponding position that is consistent with 0.1% contribution to the total spectrum at most (a blow-up of the high-bias data is given as an inset to Fig. 6). This is consistent with the weights of 2 and 4% chosen for the fit (that yield 0.08% contribution). Anyway, the mixing ratio is determined by the relative orientation of the grains and does not contain any intrinsic information. We therefore accept the aforementioned consistency as sufficient.

TWO-BAND FITTING OF SIS SPECTRA

Most tunneling work that determined Δ_L , or at least found evidence for its presence, did so by studying direct tunneling contributions from the 2D band in SIN junctions (double-peak structures). In the previous section we illustrated how such contributions do, even though rarely, influence SIS junctions. However, the more frequently seen extra feature in SIS junctions is entirely different in shape and origin. Figure 7 gives an example for a well-developed *dip* near $\Delta_S + \Delta_L$, in contrast to the *peak* at this position that we discussed before. This feature is commonly seen in our SIS junctions, and

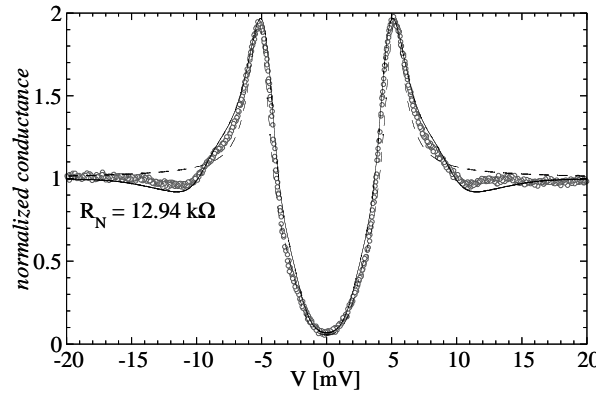


FIG. 9: Low temperature spectrum showing direct tunneling exclusively from the 3D band, and an additional dip feature near $\Delta_S + \Delta_L$. Thin dashed line is a fit to a (one-band) BCS model, solid line to a two-band model (McMillan's equations) [41].

can certainly not be explained by any parallel tunneling channel, as such extra channels should exclusively yield additional conductance.

Comparison of SIS fits and the actual data (see e.g. Fig. 4) reveals that (with increasing bias) the data first exceeds the BCS expectation and then distinctively drops below it [73], a behavior reminiscent of strong-coupling effects. However, at this energy there are very few phonons available and the electron-phonon coupling to the 3D band at any rate is expected to be weak. To establish this feature to be intimately related to superconductivity, we studied the whole background structure in more detail.

The bottom panel of Fig. 7 shows a magnification of the conductance background in the junction shown on top, displaying a variety of small structures, where the $\Delta_S + \Delta_L$ -feature by far is the most pronounced one. With increasing magnetic field, the superconducting gap structure weakens [74] and along with it, the $\Delta_S + \Delta_L$ -feature vanishes. At the same time, the other background structure remains unchanged, proving the high stability of the junction and that the $\Delta_S + \Delta_L$ -dip is closely connected to superconductivity.

We believe, that this extra feature is a signature of quasiparticle transfer between the 2D and 3D bands. To explore this, we need to abandon the simple BCS model used before and employ a slightly more elaborate DOS, taking into account the interband quasiparticle interaction. The coupling between both bands in principle may be mediated by both pair and quasiparticle transfer, however, only the quasiparticle contribution yields corrections to the spectral shape of both energy gaps. Since the original treatment of two-band superconductivity [64] only considers pair transfer, it does not suffice for our purpose. Quasiparticle transfer was included into a later theoretical two band model [65], resulting in extra

structure in each DOS at the position of the respective other gap (see Fig. 8). To keep modeling mathematically simple, we use an observation pointed out in Ref. [66], viz. that the DOS in a pure BCS two-band model [64] and the DOS in McMillan’s tunneling model of the proximity effect [67] are different only in that the latter includes both pair and quasiparticle contribution on an equal footing. This means, that the McMillan model may be used to generate the DOS in a two-band model. The model requires the solution of two simultaneous equations for the respective gap functions [67]:

$$\Delta_1(E) = \frac{\Delta_1^{\text{ph}} + \Gamma_1 \Delta_2(E) / \sqrt{\Delta_2^2(E) - (E - i\Gamma_2^*)^2}}{1 + \Gamma_1 / \sqrt{\Delta_2^2(E) - (E - i\Gamma_2^*)^2}}, \quad (4)$$

$$\Delta_2(E) = \frac{\Delta_2^{\text{ph}} + \Gamma_2 \Delta_1(E) / \sqrt{\Delta_1^2(E) - (E - i\Gamma_1^*)^2}}{1 + \Gamma_2 / \sqrt{\Delta_1^2(E) - (E - i\Gamma_1^*)^2}}, \quad (5)$$

were $\Delta_{1,2}^{\text{ph}}$ are the intrinsic pairing amplitudes in both bands, $\Gamma_{1,2}$ are scattering rates related inversely to the times spent in each band prior to scattering to the other, and $\Gamma_{1,2}^*$ are smearing parameters in both bands which were added to account for lifetime effects. These gap functions are then used to create the DOS from the standard BCS expression eqn. (2). SIS spectra are created using the usual convolution eqn. (3).

To further verify the validity of this approach, we reproduced the DOS calculated from a full two-band model [65] using McMillan’s model [67]. Fig. 8 compares both results and an almost perfect agreement is found over the entire voltage range. We therefore may safely use this model to fit our results and investigate the effects of interband quasiparticle transfer on the DOS.

Figure 9 gives an example for a typical low-temperature SIS conductance spectrum, along with a fit to the standard-BCS model used before (dashed line) and a fit using McMillan’s model (solid line). Whereas the BCS fit fails to reproduce the higher bias features, McMillan’s model results in a close fit over the entire voltage range, *including* the dip near $\Delta_S + \Delta_L$ [75]. The success of this model confirms that the $\Delta_S + \Delta_L$ -dip reflects the quasiparticle coupling in between both bands. To our knowledge, this so far is the only piece of experimental evidence from tunneling spectroscopy to not only show two gaps, but to also give direct evidence for their coupling from a detailed analysis of their spectral shape.

RULING OUT PROXIMITY EFFECTS

However, the applicability of this model *a priori* does not prove two-band superconductivity to be the origin of the dip-feature, as McMillan’s model originally was developed to describe the proximity effect, which therefore

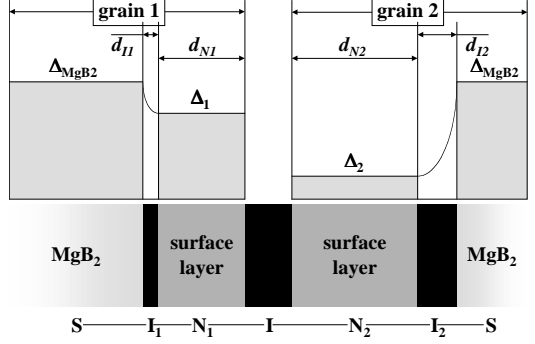


FIG. 10: Schematic representation of an asymmetric SIS’ junction caused by randomly, and non-uniformly formed surface layers. Here, the surface layers are considered part of the grains. See text for details.

needs to be considered as a possible cause. In the proximity effect, a thin surface layer of reduced (or no) intrinsic superconductivity is influenced by an adjacent superconductor to show enhanced superconductivity (or some superconductivity at all). McMillan’s equations specifically describe the proximity effect in the presence of an insulating barrier of thickness, d_I , in between the bulk superconductor and a surface layer of thickness, d_N .

Allowing for such an unknown surface layer (which in the case of MgB₂ may easily be envisioned to be e.g. MgO_x) the observation of a small gap is conceivable *without* considering two-band superconductivity. Note, that even the temperature dependence of Δ_S , or more specifically its closing at T_c , is not inconsistent with the behavior of a proximity sandwich. In spatially extended junctions (like point contacts or planar junctions) it is furthermore plausible to find more than one gap, as the surface layer may vary over the junction area (or simply not be present in some areas)—such spatial variations in sample properties over the junction area have been suggested to explain point contact data.

There are two strong arguments against this proximity scenario and in favor of two-band superconductivity. Firstly, the unusual reproducibility of the small gap’s magnitude in a wide variety of experiments using different samples and tunneling techniques. Referring again to Tab. I, it is obvious, that almost all experiments would agree to $\Delta_S = 2.0 - 2.8$ meV. To fully appreciate this agreement, one has to keep in mind how sensitively the induced gap would depend on the properties of an assumed proximity sandwich. d_N enters the induced gap with a mere power law, however, d_I , —representing a tunneling barrier—enters exponentially (for an experimental verification of this aspect of McMillan’s model, see Ref. [69]). This means, that very slight changes in the barrier thickness result in a variation of the induced gap that may easily cover several orders of magnitude.

Again, our SIS geometry allows us to strengthen this

point. Since the junction becomes rather complex in this model, we refer to the sketch in Fig. 10. In general, the SIS junction is now represented by two proximity sandwiches separated by the main barrier, I. Each sandwich in turn consists of the bulk superconductor, S, a barrier, $I_{1,2}$, and a surface layer, $N_{1,2}$. As the surface layers form randomly, there is no reason to assume the I_i and N_i to be equivalent. Likewise, the effective gap values entering the “main” SIS junction may be different, resulting in an *asymmetric SIS*’ junction.

Such junctions are known to show a unique spectral shape, including a so-called “difference peak” at $\Delta_1 - \Delta_2$ [76]. *Vice versa*, the absence of this feature (as seen in Fig. 4) gives direct evidence of the symmetry of the junction. Testing for very small asymmetries requires a detailed analysis of the in-gap spectral shape, since the difference peak (or zero-bias peak in symmetric junctions) is subject to thermal broadening—in stark contrast to the coherence peak (see Fig. 1d). Therefore, the difference peak may be veiled and show up only as a characteristic change of the in-gap spectral shape. Analyzing simulated SIS’ spectra allowing for increasing difference in gap values, we find that 20% difference is about the maximum that might still be considered consistent with our data. Using the numbers from Ref. [69], we estimate that this translates into a reproducibility of barrier thickness, $I_{1,2}$, on the order of ± 0.5 Å. Considering the initial assumption that such proximity sandwiches need to form randomly, and independently, such a reproducibility certainly proves this consideration to be highly unlikely.

A second argument against the proximity effect is the observation of both gaps simultaneously at a *single point* in STM studies, which is very hard to reconcile with the assumption of variable surface layers. Although in principle any proximity induced, small gap structure is expected to show an additional feature at the intrinsic, large gap energy, this feature is expected to be much weaker than the main, induced gap structure. It certainly is inconsistent with two peaks of equal magnitude, or even the high-bias peak being more pronounced than the low-bias peak (see e.g. data in Ref. [14]).

The appearance of two distinct gap values, the temperature dependence of the small gap, and the appearance of additional spectral features are therefore not only more easily understood in the framework of two-band superconductivity, but—beyond that—not readily consistent with the proximity effect.

CONCLUSION

We have reproducibly observed a small gap, $\Delta_S = 2.5$ meV, in break-junction tunneling on MgB₂ and traced it to high temperatures, where it closes near the bulk T_c . Only in rare cases, we also observe direct tunneling contributions showing a large gap, $\Delta_L = 7.6$ meV.

These findings give evidence for, and are interpreted in terms of a two-band model. A commonly observed dip feature at $\Delta_S + \Delta_L$ is analyzed using a specific two-band model. We argued, that this feature gives evidence for quasiparticle contributions to interband coupling, and furthermore showed it to be inconsistent with the result of proximity effects. Taken together with tunneling data from the literature, this gives very convincing evidence that MgB₂ is one of the very rare materials showing two-band superconductivity.

Acknowledgements

We are indebted to B. Jankó and C. P. Moca for valuable discussions and sharing unpublished results from their two-band calculations. We want to thank K. Scharnberg for allowing us to use Fig. 8a. We further want to thank M. A. Belogolovskii, G. Burnell, D. J. Kang, J.-I. Kye, D. Mijatovic, A. Saito, and K. Ueda for sending their manuscripts prior to publication. This research is supported by the U.S. Department of Energy, Basic Energy Sciences—Materials Sciences, under contract # W-31-109-ENG-38.

- [1] J. Nagamatsu *et al.*, Nature **410** (2001) 63.
- [2] A. Y. Liu *et al.*, Phys. Rev. Lett. **87** (2001) 087005.
- [3] I. Giaver, Phys. Rev. Lett. **5** (1960) 147.
- [4] R. C. Dynes, V. Narayanamurti and J. P. Gorno, Phys. Rev. Lett. **41** (1978) 1509.
- [5] A. F. Andreev, Zh. Éksp. Teor. Fiz. **46** (1964) 1823 [Sov. Phys. JETP **19** (1964) 1228].
- [6] G. E. Blonder, M. Tinkham and T. M. Klapwijk, Phys. Rev. B **25** (1982) 4515.
- [7] A. Pleceník *et al.*, Phys. Rev. B **49** (1994) 10016.
- [8] G. Rubio-Bollinger *et al.*, Phys. Rev. Lett. **86** (2001) 5582.
- [9] H. Suderow *et al.*, Physica C **369** (2002) 106.
- [10] A. Sharoni *et al.*, J. Phys.: Cond. Mat. **13** (2001) L503.
- [11] A. Sharoni *et al.*, Phys. Rev. B **63** (2001) 220508.
- [12] G. Karapetrov *et al.*, Phys. Rev. Lett. **86** (2001) 4374.
- [13] G. Karapetrov *et al.*, in *Studies of High Temperature Superconductors*, ed. A. V. Narlikar, (Nova Sci. Publ., New York, 2002), vol. 38, pp. 221.
- [14] M. Iavarone *et al.*, Phys. Rev. Lett. in press (cond-mat/0203329).
- [15] R. J. Olsson *et al.*, unpublished (cond-mat/0201022).
- [16] F. Giubileo *et al.*, Phys. Rev. Lett. **87** (2001) 177008.
- [17] F. Giubileo *et al.*, Europhys. Lett. **58** (2002) 764.
- [18] F. Giubileo *et al.*, Int. J. Mod. Phys. B **16** (2002) 1577.
- [19] J. Karpinski *et al.*, unpublished (cond-mat/0207263).
- [20] M. R. Eskildsen *et al.*, Phys. Rev. Lett. in press (cond-mat/0207394).
- [21] P. Seneor *et al.*, Phys. Rev. B **65** (2001) 012505.
- [22] A. Plecenik *et al.*, Physica C **368** (2001) 251.
- [23] F. Laube *et al.*, Europhys. Lett. **56** (2001) 296.

[24] A. I. D'yachenko *et al.*, unpublished (cond-mat/0201200).

[25] Z. Z. Li *et al.*, Supercond. Sci. Technol. **14** (2001) 994.

[26] Z.-Z. Li *et al.*, Phys. Rev. B **66** (2002) 064513.

[27] P. Szabó *et al.*, Phys. Rev. Lett. **87** (2001) 137005.

[28] Yu. G. Naidyuk *et al.*, Pis. Zh. Éksp. Teor. Fiz. **75** (2002) 283 [JETP Lett. **75** (2002) 238].

[29] N. L. Bobrov *et al.*, in *New Trends in Superconductivity*, ed. J. F. Annett and S. Kruchinin, (Kluwer Academic Publ., Dordrecht, 2002), vol. 67, pp. 225.

[30] I. K. Yanson *et al.*, unpublished (cond-mat/0206170).

[31] S. Lee *et al.*, Physica C **377** (2002) 202.

[32] Y. Bugoslavsky *et al.*, Supercond. Sci. Technol. **15** (2002) 526.

[33] A. Kohen *et al.*, Phys. Rev. B **64** (2001) 060506.

[34] M. A. Belogolovskii *et al.*, unpublished.

[35] R. S. Gonnelli *et al.*, J. Phys. Chem. Solids in press.

[36] R. S. Gonnelli *et al.*, unpublished (cond-mat/0208060).

[37] R. S. Gonnelli *et al.*, Int. J. Mod. Phys. B **16** (2002) 1553.

[38] R. S. Gonnelli *et al.*, Phys. Rev. Lett. **87** (2001) 097001.

[39] H. Schmidt *et al.*, Phys. Rev. B **63** (2001) 220504.

[40] H. Schmidt *et al.*, in *Studies of High Temperature Superconductors*, ed. A. V. Narlikar, (Nova Sci Publ., New York, 2002), vol. 38, pp. 229.

[41] H. Schmidt *et al.*, Phys. Rev. Lett. **88** (2002) 127002.

[42] present work.

[43] T. Takasaki *et al.*, Physica C in press.

[44] Y. Zhang *et al.*, Appl. Phys. Lett. **79** (2001) 3995.

[45] Y. Xuan *et al.*, Chin. Phys. Lett. **18** (2001) 1254.

[46] Z. Z. Li *et al.*, Physica C **370** (2002) 1.

[47] J.-I. Kye *et al.*, unpublished.

[48] D. Mijatovic *et al.*, Appl. Phys. Lett. **80** (2002) 2141.

[49] D. Mijatovic *et al.*, unpublished.

[50] A. Brinkman *et al.*, Appl. Phys. Lett. **79** (2001) 2420.

[51] G. Burnell *et al.*, Appl. Phys. Lett. **79** (2001) 3464.

[52] G. Burnell *et al.*, Appl. Phys. Lett. **81** (2002) 102.

[53] G. Burnell *et al.*, unpublished.

[54] D.-J. Kang *et al.*, unpublished (cond-mat/0206207).

[55] D.-J. Kang *et al.*, unpublished.

[56] D. K. Aswal *et al.*, Phys. Rev. B **66** (2002) 012513.

[57] M. H. Badr *et al.*, Phys. Rev. B **65** (2002) 184516.

[58] G. Carapella *et al.*, Appl. Phys. Lett. **80** (2002) 2949.

[59] A. Saito *et al.*, unpublished.

[60] K. Ueda and M. Naito, unpublished (cond-mat/0208571).

[61] H. J. Choi *et al.*, Phys. Rev. B **66** (2002) 020513(R).

[62] H. J. Choi *et al.*, Nature **418** (2002) 758.

[63] L. Ozyuzer, J. F. Zasadzinski and K. E. Gray, Cryogenics **38** (1998) 911.

[64] H. Suhl, B. T. Matthias and L. R. Walker, Phys. Rev. Lett. **3** (1959) 552.

[65] N. Schopohl and K. Scharnberg, Solid State Commun. **22** (1977) 371.

[66] C. Noce and L. Maritato, Phys. Rev. B **40** (1989) 734.

[67] W. L. McMillan, Phys. Rev. **175** (1968) 537.

[68] C. P. Moca *et al.*, unpublished.

[69] K. E. Gray, Phys. Rev. Lett. **28** (1972) 959.

[70] Enhanced gap values are more easily understood as due to strong electron-phonon coupling.

[71] Note, that assuming the same Γ for both bands the $\Delta_S + \Delta_L$ peak is intrinsically sharper than the $2\Delta_S$ peak and therefore the relative peak heights do not directly reflect the $\sim 94\%$ contribution from 3D-3D and $\sim 6\%$ from 3D-2D tunneling.

[72] The contributions to the effective total DOSs are c_{L1} , c_{L2} from the large and $c_{S1} = 1 - c_{L1}$, $c_{S2} = 1 - c_{L2}$ from the small-gapped band in the 1st and 2nd electrode, respectively. Therefore, the contribution to the conductance spectrum is $c_{S1}c_{S2}$ for the $2\Delta_S$ peak, $c_{S1}c_{L2} + c_{L1}c_{S2}$ for the $\Delta_S + \Delta_L$ peak, and finally $c_{L1}c_{L2}$ for the $2\Delta_L$ peak. Thus a sizable effect from this high-bias peak is observed only if the product of both 2D contributions is sizable.

[73] In our best junctions, the conductance indeed even drops below unity (see e.g. Fig. 7), however, in most junctions it “at least” drops below the BCS line.

[74] A detailed study of the field dependence in MgB₂ break junctions is in progress and will be reported elsewhere.

[75] Moca *et al.* developed a full two-band treatment of MgB₂ and achieved an even better agreement with the very same data [68]. However, the point of our model is to qualitatively demonstrate the necessity to include quasi-particle transfer in any theoretical model.

[76] This peak is equivalent in origin to the thermally activated zero-bias peak in symmetric junctions.